

Numerical study of the magnetic electron drift vortex mode turbulence in a nonuniform magnetoplasma

Dastgeer Shaikh,¹ B. Eliasson,^{2,3} and P. K. Shukla^{2,3,4,5,6}

¹ *Department of Physics and Center for Space Plasma and Aeronomic Research (CSPAR)
The University of Alabama in Huntsville, Huntsville. Alabama, 35899*

² *Institut für Theoretische Physik IV, Ruhr-Universität Bochum
D-44780 Bochum, Germany*

³ *Department of Physics, Umeå University, SE-901 87, Umeå, Sweden*

⁴ *Scottish Universities Physics Alliance,
Department of Physics, University of Strathclyde,
Glasgow G4 0NG, Scotland, U. K.*

⁵ *GoLP/Instituto de Plasmas e Fusao Nuclear,
Instituto Superior Técnico, 1049-001 Lisboa, Portugal*

⁶ *School of Physics, University of KwaZulu-Natal, Durban 4000, South Africa*

(Received 19 January 2008)

Abstract

A simulation study of the magnetic electron drift vortex (MEDV) mode turbulence in a magnetoplasma in the presence of inhomogeneities in the plasma temperature and density, as well as in the external magnetic field, is presented. The study shows that the influence of the magnetic field inhomogeneity is to suppress streamer-like structures observed in previous simulation studies without background magnetic fields. The MEDV mode turbulence exhibits non-universal (non-Kolmogorov type) spectra for different sets of the plasma parameters. In the presence of an inhomogeneous magnetic field, the spectrum changes to a 7/3 power law, which is flatter than without magnetic field gradients. The relevance of this work to laser-produced plasmas in the laboratory is briefly mentioned.

PACS numbers: 52.25.Gj, 52.35.Fp, 52.50.Jm, 98.62.En

I. INTRODUCTION

The generation of magnetic field in laser-produced plasmas in the laboratory [1, 3, 4, 5, 6, 7] and in the universe [8, 9, 10, 11, 12] is an fascinating and rich field of research. Possible mechanisms to spontaneously generate magnetic fields in a plasma include the Biermann battery [13], which is associated with non-parallel density and temperature gradients, and the Weibel instability [14], in which the electrons have a non-isotropic temperature. The Weibel instability may be responsible for the generation of large-scale magnetic fields in the Universe, as well as in inertial fusion plasmas [15, 16, 17], while the Biermann battery has been proposed as a possible mechanism to produce mega-Gauss magnetic fields in laser-produced plasmas [1]. There are recent observations of megagauss-field topology changes and structure formation in laser-produced plasmas [2]. The observations of spontaneous generation of magnetic fields in plasmas [1, 3] and effects attributed to self-generated magnetic fields, such as transport of energy along surfaces [18] and the insulation of laser-heated electrons from the target interior [18, 19], inspired the investigation of magnetic surface waves in plasmas [20]. This model was generalized to investigate the generation of magnetic fields from temperature and density gradients in the plasma [21]. The nonlinear properties of MEDV modes in a nonuniform plasma with the equilibrium density and electron temperature gradients have been investigated analytically without [22, 23], and with [24] background magnetic fields. The spectral and statistical properties [25], as well as the generation of large scale magnetic fields [26] by the MEDV mode turbulence, have been investigate both theoretically and numerically. The generation of steep, non-Kolmogorov spectra of streamer-like structures by MEDV turbulence has been observed in recent simulation studies [27].

In this paper, we report a simulation study of the MEDV mode turbulence in the presence of gradients in the equilibrium electron temperature and electron density, as well as in the background magnetic field. We concentrate our study on the magnetic field effect and its influence on the spectral properties of the MEDV mode turbulence. The MEDV mode turbulence involve a competition between nonlinear zonal flows [28], which we define as nonlinear MEDV modes with a finite scale in the direction of the equilibrium plasma density and temperature gradients, and streamers that have a finite scale perpendicular to the plasma gradients. We will here assume that the background magnetic field gradient is in the same direction as the plasma gradients. Our work presented here ignores collisional effects.

The latter are discussed in Ref. [29] that includes frictional and thermal forces, as well as gradients of the unperturbed magnetic field.

The manuscript is organized in the following fashion. The governing nonlinear equations for the two-dimensional (2D) MEDV modes are presented in Sec. II. The results of computer simulations are displayed in Sec. III., and the observed spectral properties of the MEDV turbulence are discussed in Sec. IV. Finally, the results are briefly summarized and discussed in Sec V.

II. NONLINEAR EQUATIONS

We here derive the governing equations for nonlinearly interacting 2D MEDV modes in an inhomogeneous plasma containing equilibrium electron density, electron temperature and background magnetic field gradients. Following Ref. [22], we will assume a 2D geometry in the xy plane, where the perturbed magnetic field is directed along the z axis so that $\mathbf{B} = B(x, y, t)\hat{\mathbf{z}}$, where $\hat{\mathbf{z}}$ is the unit vector along the z axis. The governing equations for the wave magnetic field B and electron temperature fluctuations T_1 are given by [22]

$$\frac{\partial}{\partial t} \left(\frac{e}{m} B - \frac{1}{\mu_0 e n_0} \nabla^2 B \right) = \frac{1}{(\mu_0 e n_0)^2} \{B, \nabla^2 B\} - \frac{1}{m n_0} \{n_0, T_1\} \quad (1)$$

and

$$\frac{\partial T_1}{\partial t} + \frac{1}{\mu_0 e n_0} \{B, T_0 + T_1\} + (\gamma - 1) \frac{T_0}{\mu_0 e n_0^2} \{n_0, B\} = 0, \quad (2)$$

respectively. Here e is the magnitude of the electron charge, m is the electron mass, $\mu_0 = 1/c^2 \epsilon_0$ is the magnetic permeability in vacuum, c is the speed of light, ϵ_0 the electric permittivity in vacuum, and $\gamma = 5/3$ is the ratio between the specific heats. The equilibrium electron number density n_0 and the electron temperature T_0 are assumed to have a gradient along the x axis. In Eqs. (1) and (2), we have introduced the Poisson bracket notation

$$\{f, g\} = \frac{\partial f}{\partial x} \frac{\partial g}{\partial y} - \frac{\partial f}{\partial y} \frac{\partial g}{\partial x}. \quad (3)$$

We have neglected the scalar nonlinearity [22] in Eq. (1), which becomes important only on timescales much larger than the electron gyro period [22]. On a longer timescale the effect of the scalar nonlinearity can be important, and numerical simulations [30] indicate that it causes dipolar vortices to gradually transform to monopolar vortices.

Dividing the magnetic field as $B = B_0 + B_1$, where B_0 is the large-scale background magnetic field and B_1 is the perturbations, and assuming that the equilibrium quantities n_0 , T_0 and B_0 depend only on the coordinate x , we have

$$\frac{\partial}{\partial t} \left(\frac{e}{m} B_1 - \frac{1}{\mu_0 e n_0} \nabla^2 B_1 \right) = \frac{1}{(\mu_0 e n_0)^2} (\{B_0, \nabla^2 B_1\} + \{B_1, \nabla^2 B_1\}) - \frac{1}{m n_0} \{n_0, T_1\} \quad (4)$$

and

$$\frac{\partial T_1}{\partial t} + \frac{1}{\mu_0 e n_0} (\{B_0, T_1\} + \{B_1, T_1\}) + (\gamma - 1) \frac{T_0}{\mu_0 e n_0^2} \{n_0, B_1\} = 0, \quad (5)$$

where we have used that $\{B_0, T_0\} = \{n_0, B_0\} = \{B_0, \nabla^2 B_0\} = 0$.

In order to investigate the basic properties of the nonlinear system of equations (4) and (5), it is convenient to scale it with its typical length and time scales. Noting that the characteristic length scale of the system is the electron skin depth $\lambda_e = c/\omega_{pe}$, where $\omega_{pe} = (n_0 e^2 / \epsilon_0 m)^{1/2}$ is the electron plasma frequency, and that the typical time scale is the plasma inhomogeneity length scale divided by the thermal speed of the electrons [22], it is possible to cast the system (4)–(5) into the dimensionless form

$$\frac{\partial}{\partial t} (B_1 - \nabla^2 B_1) = \{B_1, \nabla^2 B_1\} + \kappa_B \nabla^2 \frac{\partial B_1}{\partial y} - \frac{\partial T_1}{\partial y}, \quad (6)$$

and

$$\frac{\partial T_1}{\partial t} = -\{B, T_1\} - \kappa_B \frac{\partial T_1}{\partial y} - \sigma \frac{\partial B_1}{\partial y}. \quad (7)$$

where we have normalized the spatial coordinates x and y by the electron skin depth λ_e , the time by $\lambda_e / V_{Te} (|\kappa| \kappa_n)^{1/2}$, the magnetic field by $(m/e) V_{Te} (|\kappa| \kappa_n)^{1/2} / \lambda_e$, and the temperature fluctuations T_1 by $(|\kappa| \kappa_n)^{1/2} T_0$, where $V_{Te} = (T_e/m)^{1/2}$ is the electron thermal speed. The normalized background plasma gradients are given by $\kappa_n = (n'_0/n_0)(c/\omega_{pe})$, $\kappa = [(\gamma - 1)n'_0/n_0 - (T'_0/T_0)](c/\omega_{pe})$, and the normalized magnetic field gradient by $\kappa_B = (B'_0/B_0)(c/\omega_{pe})$, where the primes denote differentiation with respect to x . The coordinate system is chosen such that $\kappa_n > 0$. With this normalization, $\sigma = +1$ for $\kappa > 0$ and $\sigma = -1$ for $\kappa < 0$. Hence, the only parameters in (6) and (7) are σ and κ_B , where σ only takes the values $+1$ or -1 .

Linearizing the system of Eqs. (6) and (7), and assuming that B_1 and T_1 are proportional to $\exp(ik_x x + ik_y y - i\omega t)$, we obtain the linear dispersion relation

$$(\omega - \kappa_B k_y)[\omega + k^2(\omega - \kappa_B k_y)] = k_y^2 \sigma. \quad (8)$$

where ω and $\mathbf{k} = \hat{\mathbf{x}}k_x + \hat{\mathbf{y}}k_y$ are the frequency and wave vector, respectively. Equation (8) has solutions of the form

$$\omega = \frac{k_y}{2(1+k^2)} \left[\kappa_B(1+2k^2) \pm \sqrt{\kappa_B^2 + 4(1+k^2)\sigma} \right]. \quad (9)$$

For $\sigma = -1$, we have unstable MEDV modes for $4(1+k^2) > \kappa_B^2$ when $k_y \neq 0$. For $\sigma = +1$, we have only stable MEDV modes, and one can find zero-frequency waves when $k = 1/\kappa_B$, in addition to the zero frequency zonal flows at $k_y = 0$. In the limit $\kappa_B \rightarrow 0$ we retain the previous result [21, 22]

$$\omega = \pm \frac{k_y}{\sqrt{1+k^2}} \sqrt{\sigma}, \quad (10)$$

which predicts stable MEDV modes for $\sigma > 0$ and purely growing MEDV modes for $\sigma < 0$. The unstable case $\sigma < 0$ corresponds to a situation where density and temperature gradients are in the same direction and $(T'_0/T_0) > (\gamma - 1)n'_0/n_0$. This instability gives rise to the generation of magnetic field fluctuations and is related to the first order baroclinic ($\nabla n_0 \times \nabla T_1$) effect, which shows the importance of the temperature fluctuations for the instability to take place [21].

The nonlinear system possesses the conserved energy integral

$$\mathcal{E} = \int \int \left[B^2 + (\nabla B)^2 + \frac{T_1^2}{\sigma} \right] dx dy. \quad (11)$$

We note that the total energy is independent of κ_B . For $\sigma = +1$ the energy integral is positive definite, and thus does not allow the growing of large amplitude magnetic fluctuations from small-amplitude noise. For $\sigma = -1$, however, the energy integral is non-definite and allows large-amplitude waves to grow from the linear instability discussed above.

III. NUMERICAL STUDY

We have adapted the nonlinear fluid code that was developed to study the evolution of MEDV modes in [27] in the presence of equilibrium electron density and temperature gradients, to also include a background gradient in the magnetic field. Consequently, the energy stored in these gradients excite linear as well as nonlinear instabilities in a different manner, than that described in [27], because the nonlinear mode coupling interactions are significantly modified by the presence of both plasma and magnetic field gradients. Our

numerical code employs a doubly periodic spectral discretization of magnetic field and temperature fluctuations in terms of its Fourier components, while nonlinear interactions are de-convoluted back and forth in real and Fourier spectral spaces. The time integration is performed by using the 4th-order Runge-Kutta method. A fixed time integration step is used. The conservation of energy given by (11) is used to check the numerical accuracy and validity of our numerical code during the nonlinear evolution of the magnetic field and temperature fluctuations. Varying spatial resolution (from 128^2 to 512^2), time step ($10^{-2}, 5 \times 10^{-3}, 10^{-3}$), constant values of $K_n \lambda V_T^2 / c^2 = 0.1$ and $(2/3)K_n \lambda - K_T \lambda = 0.1$ are used to ensure the accuracy and consistency of our nonlinear simulation results. We also make sure that the initial fluctuations are isotropic and do not influence any anisotropy during the evolution. Nonlinear interactions can, however, lead to anisotropic turbulent cascades by migrating spectral energy in either $k_y \approx 0$ or $k_x \approx 0$ modes. The preference of energy transfer in either of the modes is determined primarily by the background gradients in magnetic or temperature and density fields that, in nonlinearly saturated state, govern the mode coupling interactions. In our present simulations, we largely focus on two cases, viz (i) small amplitude and (ii) large amplitude evolution of turbulent fluctuations. These two cases are characteristically different from each other in terms of dominant nonlinear interactions. To compare the effects of the amplitude we need to compare the nonlinear terms (the vector nonlinearities) with the linear terms, most importantly the coupling terms between the magnetic field and temperature fluctuations. Hence, we can compare the nonlinear term $\{B_1, \nabla^2 B_1\}$ to the coupling term $\partial T_1 / \partial y$ in the dimensionless Eq. (6). In the simulations (Figs. 1 and 2) we observed that the amplitudes of the dimensionless magnetic field and temperature fluctuations are approximately the same for both the small and large amplitude cases when the turbulence is fully developed. Hence we may use $T_1 \sim B_1$ and compare the nonlinear term $\{B_1, \nabla^2 B_1\}$ to $\partial B_1 / \partial y$. As an order of magnitude estimate, the spatial derivatives are of the order $1/L$, where L is the typical length scale of the fluctuations. Hence we have the order of magnitude estimates $|\{B_1, \nabla^2 B_1\}| \sim (1/L)^4 |B_1|^2$ and $|\partial B_1 / \partial y| \sim (1/L) |B_1|$. One can conclude that if $B_1 \ll L^3$ then the linear coupling term dominates and we have a case of weak turbulence, while if $B_1 \approx L^3$ or larger, then we have a fully nonlinear case with strong turbulence. In our simulations, the fluctuations have typical length-scales of $L \approx 1$ (corresponding to the electron skin depth in dimensional units) so that $|B_1| \ll 1$ constitutes a weakly nonlinear case while $B \sim 1$ is a strongly nonlinear case.

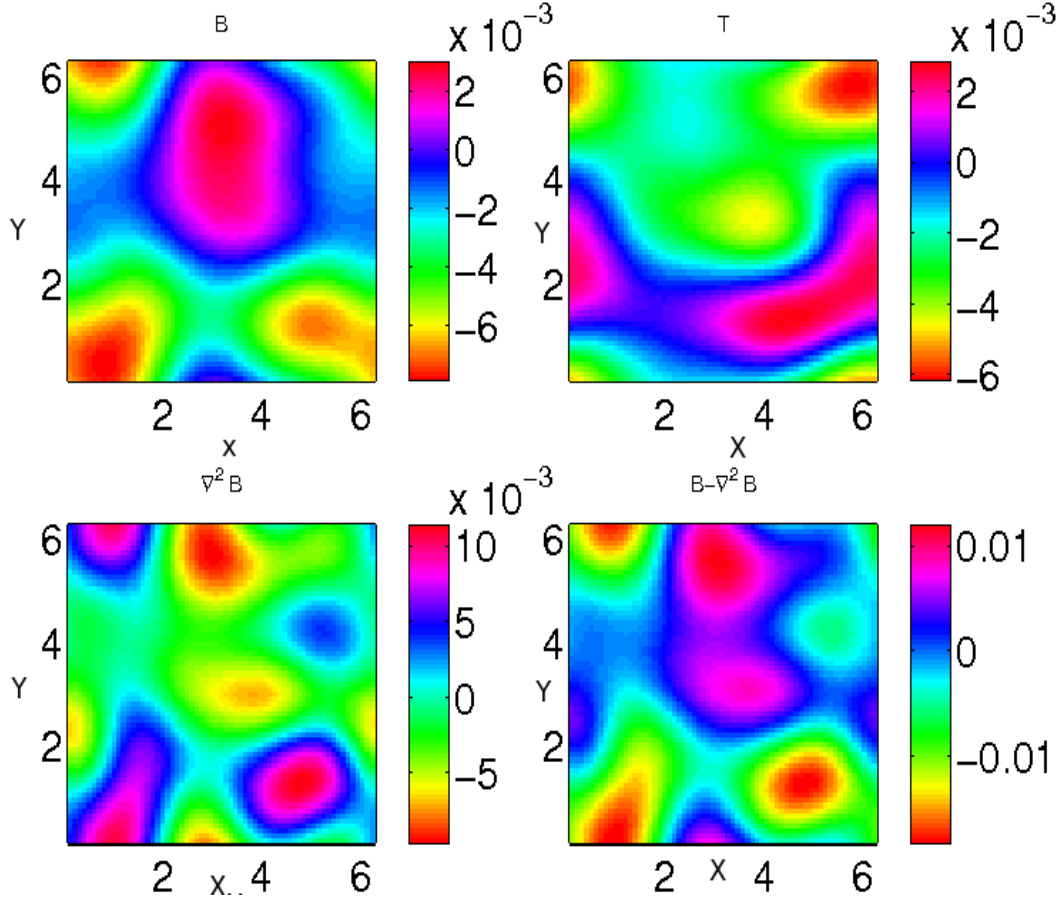


FIG. 1: (Color online) Evolution of random turbulent fluctuations initialized with small amplitude. Nonlinear turbulent interactions lead to the formation of relatively large-scale flow directed along the mean magnetic field in our 2D simulations. The saturated structures in B , T , $\nabla^2 B$ and $B - \nabla^2 B$ are shown in the figure. The numerical resolution is 256^2 , box dimension is $2\pi \times 2\pi$, and the parameters used are $\sigma = +1$ and $\kappa_B = 0.5$.

In dimensional units, B_1 should be replaced by $(eB_1/m)\lambda_e/[V_{Te}(|\kappa|\kappa_n)^{1/2}]$ and L by L/λ_e so that $e|B_1|/m$ should be compared to $(V_{Te}/\lambda_e)(|\kappa|\kappa_n)^{1/2}(L/\lambda_e)^3$ in dimensional units. Since $L/\lambda_e \approx 1$, we then have the weakly nonlinear case $e|B_1|/m \ll (V_{Te}/\lambda_e)(|\kappa|\kappa_n)^{1/2}$ and the strongly nonlinear case $e|B_1|/m \approx (V_{Te}/\lambda_e)(|\kappa|\kappa_n)^{1/2}$ in dimensional units.

The initial spectral distribution in the magnetic and temperature fluctuations comprises a uniform isotropic and random amplitude associated with the Fourier modes confined to a smaller band of wave number ($k < 0.1 k_{max}$). While spectral amplitude of the fluctuations is random for each Fourier coefficient; it follows a k^{-1} or k^{-2} scaling. Note again that our

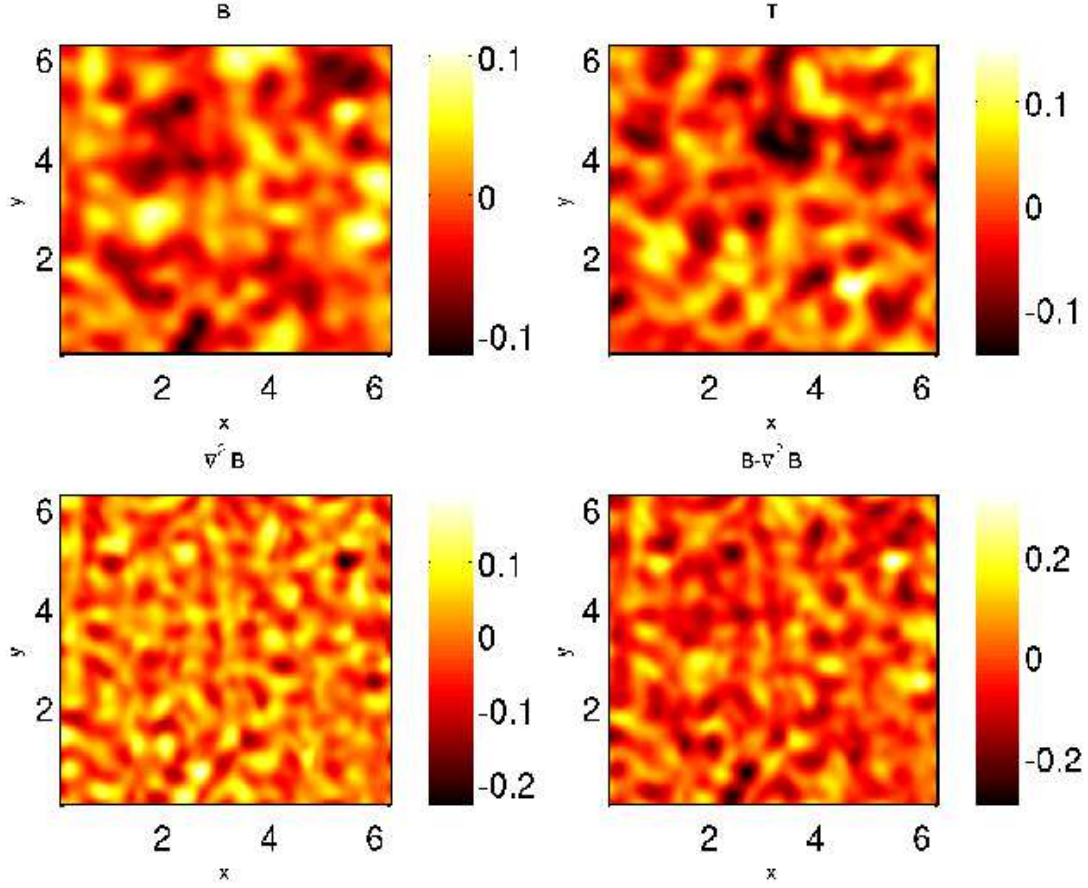


FIG. 2: (Color online) When the amplitude of initial fluctuations in magnetic and temperature fields is large enough, characteristic nonlinear interaction modify the flows observed in Fig (1). The diamagnetic-like nonlinear interactions seem to dominantly suppress the flow and lead to small scale isotropic turbulent fluctuations. This is shown in B , T , $\nabla^2 B$ and $B - \nabla^2 B$.

final results do not depend on the choice of the initial spectral distribution. The spectral distribution set up in this manner initializes random scale turbulent fluctuations. Since there is no external driving mechanism considered in our simulations, turbulence evolves freely under the influence of self-consistent nonlinear interactions. Note however that driven turbulence in the context of the MEDV mode will not change inertial range spectrum to be described here. The driving mechanism helps sustain turbulent interactions without modifying the inertial range turbulent cascades. The initial isotropic fluctuations in magnetic and temperature fields are evolved through nonlinear fluid Eqs. (6) & (7). The dominant nonlinear interactions in the inhomogeneous MEDV modes are governed by $\hat{z} \times \nabla B \cdot \nabla \nabla^2 B$ in

magnetic field equation. This nonlinearity is similar to the polarization drift nonlinearity $\hat{z} \times \nabla \phi \cdot \nabla \nabla^2 \phi$, ϕ being the electrostatic potential fluctuations, in a two dimensional Hasegawa-Mima-Wakatani (HMW) model describing drift waves in inhomogeneous plasmas [31, 32, 33, 34]. This nonlinearity characterizes Reynolds stress forces that plays a critical role in the formation of zonal-flows. Analogously, one can expect generation of nonlinearly generated flows in underlying MEDV model here. The temperature evolution, on the other hand, is governed by $\hat{z} \times \nabla T \cdot \nabla B$ nonlinearity that is identical to a diamagnetic nonlinear term in HMW model. The role of this nonlinearity has traditionally been identified as a source of suppressing the intensity of nonlinear flows in drift wave turbulence. Nevertheless, the presence of the linear inhomogeneous background in both equations can modify the nonlinear mode coupling interactions in a subtle manner. Our objective is to understand the latter in the context of nonlinear interactions mediated by the inhomogeneous B and T fields in MEDV modes.

We find from our small amplitude nonlinear evolution case (see Fig 1) that the nonlinear interactions in the inhomogeneous MEDV modes are typically led by the Reynolds-stress-like nonlinearity, i.e. $\hat{z} \times \nabla B \cdot \nabla \nabla^2 B$, in the magnetic field equation. Consequently, the mode structures in the saturated turbulent state are dominated by the zonal-like flows, as typically observed in the Hasegawa-Mima-Wakatani (HMW) model [31, 32, 33, 34]. This is demonstrated in Fig. (1) where large scale structures (zonal flow-like, $k_y \approx 0$) along the background magnetic and temperature field gradients are developed in $B, T, \nabla^2 B$ and $B - \nabla^2 B$ fluctuations. Thus, small amplitude nonlinear evolution, as shown in Fig. (1), is consistent with the HMW model of the inhomogeneous drift-wave turbulence. Our simulations described in Fig. (1) can be contrasted with our previous work [27] on the small amplitude case that was studied in the absence of a background magnetic field gradient. In Ref [27], we have shown that mode coupling interactions during the nonlinear stage of evolution leads to the formation of streamer-like structures in the magnetic field fluctuations associated with $k_y \approx 0, k_x \neq 0$. These structures were similar to the zonal flows but contained a rapid k_x variations, thus the corresponding frequency is relatively large. The temperature fluctuations in Fig (1) of [27], on the other hand, depict an admixture of isotropically localized turbulent eddies and a few stretched along the direction of the background inhomogeneity. Clearly, the presence of a background magnetic field gradient reduces the k_x variation in the steady-state flow. This leads to a considerable modification

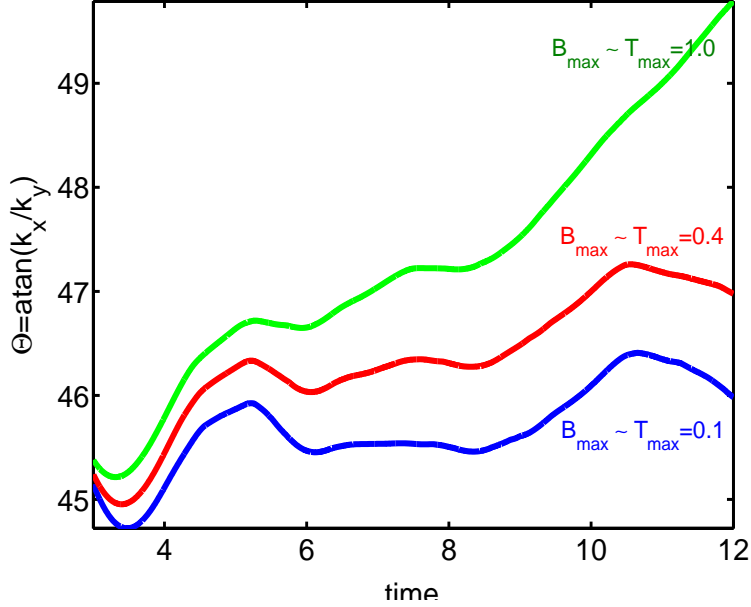


FIG. 3: (Color online) Evolution of anisotropic mode structures as described by k_x and k_y mode averaged over the entire turbulent spectrum in inhomogeneous MEDV turbulence. Initially, $k_x = k_y$. Progressive development of anisotropy $k_x > k_y$ is ascribed to the presence of background gradients in magnetic and temperature fields for which the anisotropy angle $\Theta = \tan^{-1}(k_x/k_y)$ deviates continually from 45° .

in the final structures, which now appear to look like zonal-flows (and not the streamers that were observed in the absence of a background magnetic field). Interestingly, the large amplitude case in our simulations unravels a completely different scenario where nonlinear mode coupling interactions in MEDV modes are observed to suppress the steady-state flow. This is shown in Fig. (2). The suppression of the zonal flow-like structures can be understood in the context of the diamagnetic-like nonlinearity that seems to modify the nonlinear mode coupling interactions in the large amplitude evolution. This nonlinearity, corresponding to a $\{T, B\}$ term in the temperature equation, becomes gradually strong enough to nullify the emergence of the large scale zonal-flow-like structures. Hence, the steady state structures in Fig. (2) appear to possess more small scale fully developed turbulent fluctuations. We confirm that this state is not entirely isotropic and the background gradients nonlinearly maintain the anisotropic cascades in inhomogeneous MEDV modes. We elucidate this point in the following section.

IV. ANISOTROPIC MEDV CASCADES

We quantify the degree of anisotropy mediated by the presence of large scale gradients in the magnetic and temperature fields in the nonlinear 2D inhomogeneous MEDV turbulence. In 2D turbulence, the anisotropy in the $k_x - k_y$ plane is associated with the preferential transfer of spectral energy that empowers either of the k_x and k_y modes. The anisotropy in the initial isotropic turbulent spectrum is triggered essentially by the background anisotropic gradients that nonlinearly migrate the spectral energy in a particular direction. To measure the degree of anisotropic cascades, we employ the following diagnostics to monitor the evolution of k_x mode in time. The k_x mode is determined by averaging over the entire turbulent spectrum that is weighted by k_x .

$$k_x(t) = \sqrt{\frac{\sum_k |k_x Q(k, t)|^2}{\sum_k |Q(k, t)|^2}}$$

Here Q represents any of B , T , $\nabla^2 B$ and $B - \nabla^2 B$. Similarly, the evolution of k_y mode is determined by the following relation.

$$k_y(t) = \sqrt{\frac{\sum_k |k_y Q(k, t)|^2}{\sum_k |Q(k, t)|^2}}$$

We can define an angle of anisotropy such that $\Theta = \tan^{-1}(k_x/k_y)$. It is clear from these expressions that the k_x and k_y modes exhibit isotropy when $k_x \simeq k_y$ for which $\Theta \simeq 45^\circ$. Any deviation from this equality leads to a spectral anisotropy. We follow the evolution of k_x and k_y modes in our simulations for increasing amplitude of the initial fluctuations. Our simulation results describing the evolution of k_x and k_y modes are shown in Fig. 3. It is evident from Fig. 3 that the initial isotropic modes $k_x \simeq k_y$ gradually evolve towards an highly anisotropic state in that spectral transfer preferentially occurs in the k_x mode, while the same is suppressed in k_y mode. Consequently, the spectral transfer in k_x mode dominates the evolution and the mode structures show elongated structures along the y -direction. With the increasing amplitude of the initial fluctuations, there exists increasing degree of anisotropy as illustrated in Fig 3. The larger the amplitude is, stronger are the nonlinear interactions. Correspondingly, there exists increasing degree of disparity in the k_x and k_y modes owing primarily to the increasing depletion in k_y modes as shown in Fig 3.

The increasing angle of anisotropy (in Fig 3), with the increasing magnitude of the initial fluctuations, is ascribed to the generation of highly asymmetric flows in our simulations. We

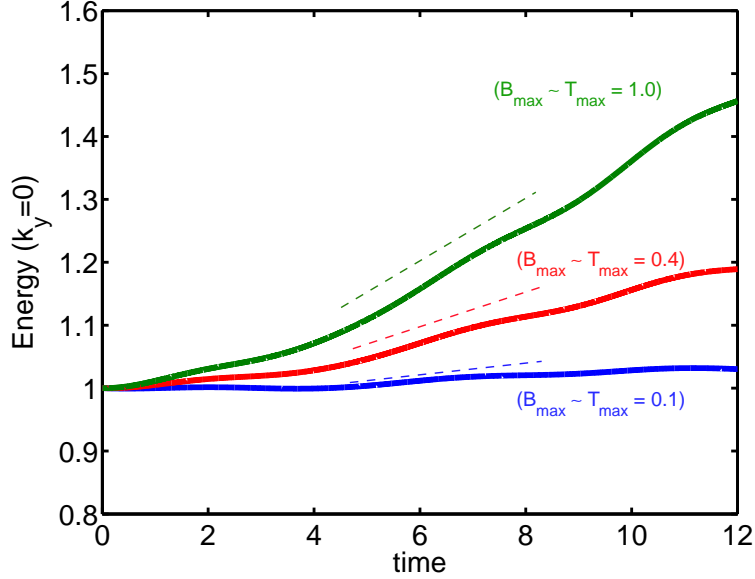


FIG. 4: (Color online) Energy associated with the anisotropic flows that corresponds essentially to the nonlinear $k_y = 0$ modes. Figure depicts the self-consistently generated nonlinear flows lead to turbulent anisotropy. The growth rate of the generation of anisotropic flow is directly proportional to the amplitude of the initial fluctuations.

exemplify this point by means of Fig 4 that describes evolution of the energy associated with the anisotropic flows led predominantly by the $k_y = 0$ mode. Notably, this mode is generated explicitly by the nonlinear interactions. It is clear from this figure that growth rate of the generation of the anisotropic (dominated by the $k_y = 0$ mode) flow is directly proportional to the magnitude of the initial fluctuations. Thus the growth rate is higher when the amplitude of the magnetic and temperature field is large, i.e. $B_{max} \simeq T_{max} = 1.0$. The smaller initial amplitude of the fluctuations correspond to relatively weak nonlinear interactions for which the generation of the $k_y = 0$ mode is insignificant. The nonlinear interactions do not introduce anisotropy and hence lead to nearly isotropic turbulent cascades. This is observed clearly in Fig 4 (see the curve corresponding to $B_{max} \simeq T_{max} = 0.1$) which is consistent with the corresponding curve in Fig 3. In Fig 4, each curve is normalized with it's own initial value to rescale all the curves on a single plot. This further enables us to make a vis a vis comparison between the three different cases shown in Fig 4. Also evident from the figure 4 is the large amplitude fluctuations that lead to the higher growth rate of the

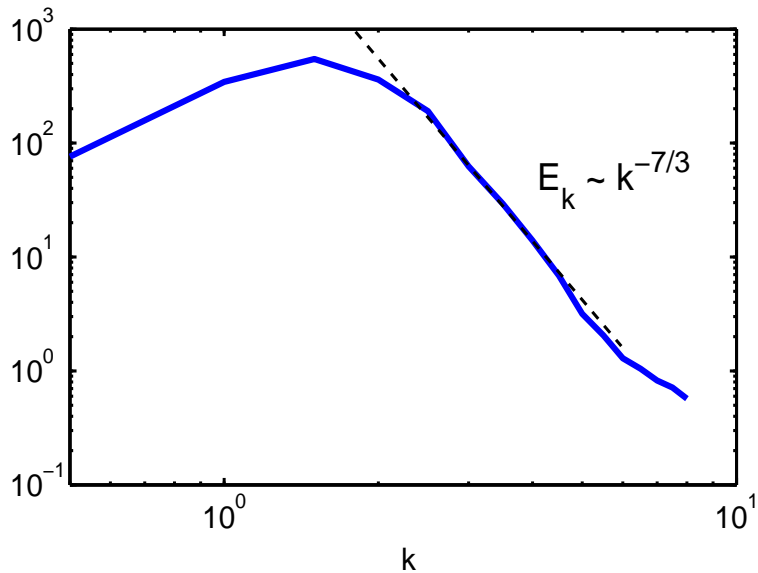


FIG. 5: (Color online) Anisotropic inhomogeneous MEDV turbulent fluctuations exhibit a $k^{-7/3}$ like spectrum. The spectrum corresponds to an intermittent state where turbulence coexists with anisotropic structures.

anisotropic flows (see dashed lines whose slope increases with the increasing amplitude of B_{max} and T_{max}). The increasing slope, i.e. growth, associated with the anisotropic flows in our simulations is further consistent with the increasing angle of anisotropy that is observed in Fig 3.

It is noteworthy from our simulations that the stronger nonlinear interactions pile up an increasing amount of turbulent energy in the $k_y = 0$ mode. Consequently, the turbulent correlation length scales tend to decrease across the flows. Hence the large amplitude simulations show decorrelated flow structures in Fig 2. This physically means that the nonlinear interactions led by the polarization and diamagnetic like terms in the presence of background gradients quench the flow (that was observed along the x -direction in Fig. 1) to introduce reduced turbulent decorrelated structures.

While there exists a disparity in the spectral transfer of energy corresponding to the k_x and k_y modes, the 2D volume averaged turbulent spectrum follows a $k^{-7/3}$ power law, as shown in Fig. (5). This spectrum is steeper than that of the HMW turbulence [31, 32, 33, 34]. The steepness of the observed spectrum can be ascribed to the coexistence of partially anisotropic flows and turbulent fluctuations in the steady state MEDV mode turbulence.

V. SUMMARY AND CONCLUSIONS

In summary, we have investigated the properties of the MEDV mode turbulence nonuniform magnetoplasma containing gradients in the electron temperature, the electron number density, and the external magnetic field. We find that the influence of the magnetic field gradient is to suppress the streamer-like structures observed in simulations without the magnetic field gradient [27]. In addition, the steep spectra changes to spectra with a $7/3$ power law in the presence of the magnetic field gradient. We also discussed the conditions for an instability through a first order baroclinic effect, which would lead to the generation of magnetic fields under conditions where the background density and temperature gradients are in the same direction. It is noteworthy that the anisotropic terms in our simulations become important when the linear terms, corresponding to the gradients in magnetic and temperature fields, compete with the nonlinear terms. In such case, efficient migration of energy takes place between the gradients and turbulent modes that primarily lead to the nonlinear anisotropic flows. Our study could have relevance for laser produced plasmas in the laboratory, spontaneously generated magnetic fields, and effects associated with self-generated magnetic fields such as transport of energy along surfaces and flux limitation of electrons, have been observed for many years.

Acknowledgments This research was partially supported by the Swedish Research Council (VR) and by the Deutsche Forschungsgemeinschaft through the Forschergruppe FOR 1048. Dastgeer Shaikh acknowledges the support of NASA(NNG-05GH38) and NSF (ATM-0317509) grants.

-
- [1] J. A. Stamper *et al.*, Phys. Rev. Lett. **26**, 1012 (1971).
- [2] C. K. Li *et al.*, Phys. Rev. Lett., 99, 055001, (2007).
- [3] A. Raven, O. Willi, and P. T. Rumsby, Phys. Rev. Lett **41**, 554 (1978).
- [4] J. A. Stamper, Laser Part. Beams **9**, 841 (1991).
- [5] M. Tatarakis *et al.*, Nature (London) **415**, 280 (2002).
- [6] M. Tatarakis *et al.*, Phys. Plasmas **9**, 2244 (2002); *ibid.* **9**, 3642 (2002); V. I. Berezhiani *et al.*, Phys. Rev. A **46**, 6608 (1992).
- [7] U. Wagner *et al.*, Phys. Rev. E **70**, 026401 (2004).
- [8] D. Grasso and H. R. Rubenstein, Phys. Rep. **348**, 163 (2001).
- [9] P. Kronberg, Phys. Plasmas **10**, 1985 (2003)
- [10] R. Schlickeiser and P. K. Shukla, Astrophys. J. Lett., **599**, L57 (2003).
- [11] R. M. Kulsrud and E. G. Zweibel, Rep. Prog. Phys. **71**, 046901 (2008).
- [12] D. Ryu, H. Kang, J. Cho, and S. Das, Science **320**, 909 (2008).
- [13] L. Biermann, Z. Naturforsch. **5A**, 65 (1950).
- [14] E. S. Weibel, Phys. Rev. Lett. **2**, 83 (1959).
- [15] L. O. Silva, R. A. Fonseca, J. W. Tonge, W. B. Mori, and J. M. Dawson, Phys. Plasmas **9**, 2458 (2002).
- [16] R. A. Fonseca, L. O. Silva, J. M. Tonge, W. B. Mori, and J. M. Dawson, Phys. Plasmas **10**, 1979 (2003).
- [17] M. V. Medvedev, L. O. Silva, and M. Kamionkowski, Astrophys. J. **642**, L1 (2006).
- [18] D. W. Forslund and J. U. Brackbill, Phys. Rev. Lett. **48**, 1614 (1982).
- [19] C. E. Max, W. N. Manheimer, and J. J. Thomson, Phys. Fluids **21**, 128 (1978).
- [20] R. D. Jones, Phys. Rev. Lett. **51**, 1269 (1983).
- [21] M. Y. Yu and L. Stenflo, Phys. Fluids **28**, 3477 (1985).
- [22] J. Nycander, V. P. Pavlenko, and L. Stenflo, Phys. Fluids **30**, 1367 (1987).
- [23] J. Nycander and V. P. Pavlenko, Phys. Fluids B **3**, 1386 (1991).
- [24] G. Murtaza *et al.*, J. Plasma Phys. **41**, 257 (1989).
- [25] V. P. Pavlenko and L. Uby, Phys. Plasmas **1**(7), 2140 (1994); M. Jucker, Zh. N. Andrushchenko and V. P. Pavlenko, Phys. Plasmas **13**, 072308 (2006); M. Jucker and V. P. Pavlenko, Phys.

- Plasmas **14**, 032303 (2007); M. Jucker and V. P. Pavlenko, Phys. Plasmas **14**, 102313 (2007); Zh. N. Andrushchenko, M. Jucker, and V. P. Pavlenko, J. Plasma Phys. **74**(1), 21 (2008).
- [26] Zh. N. Andrushchenko and V. P. Pavlenko, Phys. Plasmas **11**, 1402 (2004).
- [27] D. Shaikh and P. K. Shukla, J. Plasma Phys. **75**, 133 (2009).
- [28] P. K. Shukla *et al.*, Phys. Rev. A **23**, 321 (1981); P. K. Shukla *et al.*, Phys. Rep **105**, 227 (1984).
- [29] M.Y. Yu et al., Phys. Rev. A **40**, 5860 (1989)
- [30] L. A. Mikhailovskaya, Fiz. Plasmy **12**, 879 (1986). [Sov. J. Plasma Phys. **12**, 507 (1986).]
- [31] Hasegawa, A., and K. Mima, *Phys. Rev. Lett.* **39**, 205 (1977); K. Mima and A. Hasegawa, *Phys. Fluids* **21**, 81 (1978).
- [32] A. Hasegawa and M. Wakatani, *Phys. Rev. Lett.* **50**, 682 (1983); *ibid.* **59**, 1581 (1987).
- [33] A. Hasegawa, *Adv. Phys.* **34**, 1 (1985).
- [34] W. Horton and A. Hasegawa, A., *Chaos* **4**, 227 (1994).